Geomechanics and Engineering, *Vol. 15, No. 3 (2018) 889-898*
DOI: https://doi.org/10.12989/gae.2018.15.3.889

An analytical solution for estimating the stresses in vertical backfilled stopes based on a circular arc distribution

El-Mustapha Jaouhar[1,2a], Li Li[*1,2] and Michel Aubertin[1,2b]

[1]*Research Institute on Mines and Environment (RIME UQAT-Polytechnique)*
[2]*Department of Civil, Geological and Mining Engineering, École Polytechnique de Montréal, C.P. 6079, Succursale Centre-Ville, Montréal, QC, H3C 3A7, Canada*

(Received June 15, 2017, Revised March 2, 2018, Accepted March 23, 2018)

Abstract. Backfilling of mine stopes with waste rocks or tailings is commonly done to enhance ground stability. It is also an alternative for mining wastes disposal. A successful application of underground backfilling requires an accurate evaluation of the stress distribution in stopes. Over the years, various analytical solutions have been proposed to assess these stresses. Most of them were based on the arching theory, considering uniform stresses across horizontal layer elements. The vertical and horizontal stresses in vertical stopes are principal stresses only along the vertical center line, but not close to the walls where there is rotation of the principal stresses. A few solutions use arc layer elements that follow the iso-contours of the minor principal stresses, based on numerical solutions. In this paper, a modified analytical solution is developed for the stresses in vertical backfilled stopes, considering a circular arc distribution. The proposed solution is calibrated with a few numerical modeling results and then validated by additional numerical simulations under different conditions.

Keywords: backfill; arching effect; analytical solution; stresses; arc layer element

1. Introduction

Stope backfilling is often used in mining operations to enhance environmental protection and improve ground stability (Aubertin *et al.* 2002, Ning *et al.* 2017). A critical issue is then related to the stresses in backfilled stopes, which depend on the load transfer that may occur between the backfill and the confining rock walls. When a deformable granular material is placed within a stiffer confining structure, the soft material tends to yield and settle downward. This settlement can generate shear stresses along the confining walls. Part of the vertical load within the filling material is then transferred to the walls, reducing the stresses within the opening. This phenomenon is known as arching.

An arching theory with a specific solution was proposed by Janssen (1895) for calculating the stresses in bulk (granular) materials such as grains, cement, and coal stored in silos (e.g., Cowin 1977, Hartlen *et al.* 1984, Blight 1986, Ooi and Rotter 1990). The first application of this theory in geotechnical engineering is mainly due to Marston (1930) who developed an analytical solution for assessing the load on conduits buried in trenches (e.g., Spangler 1962, Handy 1985, McCarthy 1988). Terzaghi (1943) also used this arching theory to evaluate the soil pressure above an excavation (tunnel), based on the "trap-door" phenomenon (e.g., Ladanyi and Hoyaux 1969, Atkinson *et al.* 1974, Ono and Yamada 1993, Moradi and Abbasnejad 2015). Other applications of arching theory include solutions for the stress state on retaining walls (Handy 1985, Harrop-Williams 1989, Take and Valsangkar 2001, Paik and Salgado 2003, Dalvi and Pise 2008, Goel and Patra 2008), in dams with a soft clay core (Kutzner 1997), and in mine backfilled stopes (e.g., Askew *et al.* 1978, Knutsson 1981, Aubertin 1999, De Souza and Dirige 2002, Aubertin *et al.* 2003, Li *et al.* 2003, 2005, 2007, Caceres 2005, Pirapakaran and Sivakugan 2006, 2007a, b, Li and Aubertin 2008, 2009a, b).

The Marston (1930) solution for the load (force) on a buried conduit was obtained by considering the global equilibrium of thin, flat and horizontal elements (e.g., McCarthy 1988, Aubertin *et al.* 2003). This solution can be expressed as follows for the corresponding 2D (plane strain) stresses in a vertical backfilled opening (Aubertin *et al.* 2003)

$$\sigma_v = \frac{B\gamma}{K\tan\phi}\left[1-\exp\left(-\frac{K\tan\phi}{B}z\right)\right] \tag{1}$$

$$\sigma_h = K\sigma_v = \frac{B\gamma}{\tan\phi}\left[1-\exp\left(-\frac{K\tan\phi}{B}z\right)\right] \tag{2}$$

where σ_v (kPa) and σ_h (kPa) are the vertical and horizontal normal stresses, respectively; B (m) is the half width of the opening; γ (kN/m^3) is the unit weight of the backfill; ϕ (°) is the internal friction angle of the fill material; z (m) is the depth; $K(=\sigma_h/\sigma_v)$ is a ratio of the horizontal to the vertical stresses (usually called earth pressure coefficient).

∗Corresponding author, Associate Professor
E-mail: li.li@polymtl.ca
[a]Ph.D. Student
[b]Emeritus Professor

ISSN: 2005-307X (Print), 2092-6219 (Online)

In reality, the shear stresses induced away from the center line of the opening (with a maximum near the walls) influence the stress distribution in the fill so the vertical stresses are not uniform across the width. Eq. (1) does not reflect this variation of the stresses between the center and the side walls. Modifications to this solution can take into account results from numerical analyses, which have indicated that the trajectory of the minimum principal stress σ_3 tends to follow an arch (e.g., Sokolovoski 1965, Li *et al.* 2003, Li and Aubertin 2008). It would then be more appropriate to consider the equilibrium of a curved thin element to develop the solution rather than a flat, horizontal layer element.

Another limitation of Eqs. (1) and (2), based on Marston's approach, is related to the use of a constant value for the earth pressure coefficient K. The value of K in backfilled openings is usually taken as the Rankine's active coefficient K_a or Jaky's (1944) at-rest earth pressure coefficient K_0. The shear stresses created near the walls tends to produce a rotation of the normal stresses, so the horizontal and vertical normal stresses differ from the principal stresses at these locations (Yang *et al.* 2017a). The stress ratio K can then take a different value at different locations in the opening.

Handy (1985) considered a parabolic layer element along which there is no shear stress and the principal stresses are uniformly distributed in the backfilled opening. Later, Harrop-Williams (1989) noted that Handy's parabola distribution can be approached closely by a circular arc. Singh *et al.* (2011) considered a circular arc layer element for estimating the stresses in backfilled stopes. The latter analytical solution is based on a downward concave trajectory for the principal stresses. Results from numerical simulations however indicate that this trajectory rather follows an upward concave shape as will be shown below (see also Li *et al.* 2003, Li and Aubertin 2008). In addition, the solution proposed by Singh *et al.* (2011) was expressed in a local coordinate system, rather than in a global Cartesian system; several transformations may thus be necessary to obtain the stresses away from the center line.

In this paper, an analytical solution is developed and applied to estimate the stresses in a vertical backfilled stope by considering the equilibrium of a circular arc layer element. This work thus extends and modifies earlier solutions proposed by Handy (1985), Harrop-Williams (1989) and Singh *et al.* (2011). This alternative solution is compared with existing solutions and numerical modeling results.

2. Formulation based on arc layer element

The distribution of the minor principal stresses (σ_3) in a backfilled opening, obtained numerically by Sokolovoski (1965), was used by Handy (1985) to develop a solution that represents the curved pattern as a parabola (also called catenary). Harrop-Williams (1989) showed that this distribution of the minor principal stress can be approximated by a circular arc, expressed as follows

$$Y = \frac{1 - [1 - (\lambda X)^2]^{0.5}}{\lambda} \tag{3a}$$

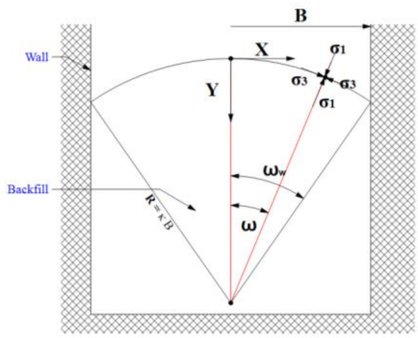

Fig. 1 An arc diagram for the stress in a vertical backfilled opening (adapted from Harrop-Williams 1989).

or

$$X^2 + \left(Y - \frac{1}{\lambda}\right)^2 = \left(\frac{1}{\lambda}\right)^2 \tag{3b}$$

where X (m) and Y (m) are the abscise and ordinate of the local coordinate system associated with the arc, respectively (Fig. 1); λ (m^{-1}) represents the curvature of the circle (Harrop-Williams 1989)

$$\lambda = \frac{1}{R} = \frac{1}{\kappa B} \tag{4}$$

where R (m) is the radius of the circle; B (m) is again the half width of the vertical opening; $\kappa (= R/B)$ is a ratio of the circle diameter ($2R$) to the stope width ($2B$). Parameter κ was expressed as a function of the internal friction angle of the fill ϕ (°) by Harrop-Williams (1989)

$$\kappa = \frac{1}{\sin(45° - \phi/2)} \tag{5}$$

From Eq. (3), the slope of the circular arc can be expressed at each point by

$$\frac{dY}{dX} = tan[sin^{-1}(\lambda X)] = tan\,\omega \tag{6}$$

where ω (°) is an angle between the major principal stress σ_1 and the vertical axis

$$\omega = \sin^{-1}\left(\frac{X}{B\kappa}\right) \tag{7}$$

Its value along the walls (i.e. $X = B$) becomes

$$\omega_w = \sin^{-1}\left(\frac{1}{\kappa}\right) \tag{8}$$

In the following sections, this circular arc shape, also used by Harrop-Williams (1989) and Singh *et al.* (2011), serves to develop an alternative analytical solution to evaluate the stresses within vertical backfilled openings.

3. Solution for the stresses in a vertical stope

Fig. 2 schematically shows a vertical backfilled stope, having a backfill height H (m) and a width $2B$ (m), with a circular arc element of thickness dz (with a downward curvature). Its position in the stope is defined by depth z

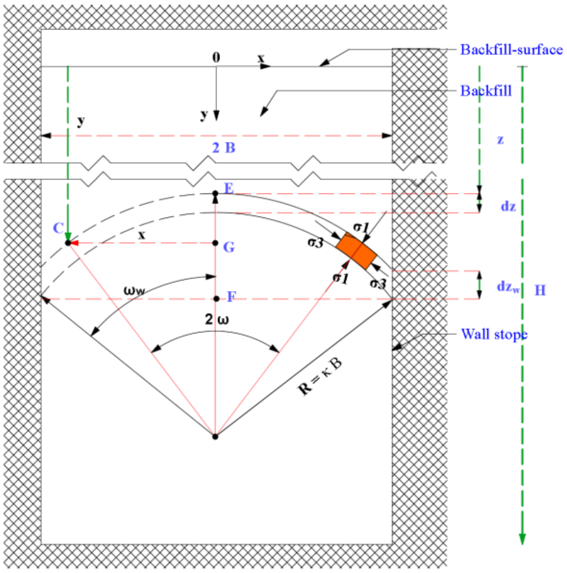

Fig. 2 A vertical backfilled stope with a circular arc layer element and the principal stresses (modified from Singh *et al.* 2011)

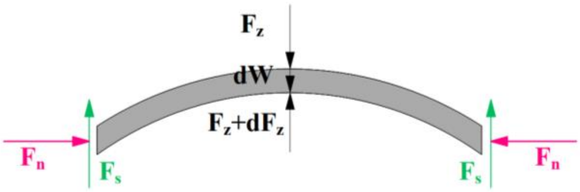

Fig. 3 A continuous compression arc element diagram with the corresponding forces

(m) of the top point E (see Fig. 2).

The vertical ($\sigma_{z,\omega}$) and horizontal ($\sigma_{X,\omega}$) normal stresses at a point along the circular arc (characterised by angle ω (°)) can be expressed from the major (σ_1) and minor (σ_3) principal stresses, using general expressions provided by McCarthy (1993), Das (1998), and others. The followings are then obtained

$$\begin{aligned}\sigma_{z,\omega} &= \frac{\sigma_1+\sigma_3}{2}+\frac{\sigma_1-\sigma_3}{2}\cos 2\omega \\ &= \sigma_1\left(\frac{1+K_{ps}}{2}+\frac{1-K_{ps}}{2}\cos 2\omega\right) \\ &= \sigma_1\left(\cos^2\omega+K_{ps}\sin^2\omega\right)\end{aligned} \tag{9}$$

$$\begin{aligned}\sigma_{X,\omega} &= \frac{\sigma_1+\sigma_3}{2}-\frac{\sigma_1-\sigma_3}{2}\cos 2\omega \\ &= \sigma_1\left(\frac{1+K_{ps}}{2}-\frac{1-K_{ps}}{2}\cos 2\omega\right) \\ &= \sigma_1\left(\sin^2\omega+K_{ps}\cos^2\omega\right)\end{aligned} \tag{10}$$

where K_{ps} is a ratio of the minor to major principal stresses

$$K_{ps} = \sigma_3/\sigma_1 \tag{11a}$$

Various analyses have indicated that K_{ps} is often close to the Rankine's active earth pressure coefficient (Li *et al.* 2003, Li and Aubertin 2009a, b, Ting *et al.* 2012, Sobhi *et al.* 2017). It can thus be expressed as follows

$$K_{ps} = K_a = \tan^2(45° - \phi/2) \tag{11b}$$

Using $\omega = \omega_w$ in Eq. (10), the horizontal normal stress on the walls σ_{hw} (kPa) becomes

$$\sigma_{hw} = \sigma_1\left(\sin^2\omega_w + K_{ps}\cos^2\omega_w\right) \tag{12}$$

For a backfill that obeys the Coulomb yield/failure criterion without cohesion, the shear strength τ_{sw} (kPa) along the walls is given by

$$\tau_{sw} = \sigma_{hw}\ \tan\delta \tag{13}$$

where δ (°) is the friction angle along the interfaces between the backfill and rock walls. Substituting Eq. (12) in Eq. (13) gives

$$\tau_{sw} = \left[\sigma_1\left(\sin^2\omega_w + K_{ps}\cos^2\omega_w\right)\right]\tan\delta \tag{14}$$

For relatively planar smooth surfaces, the value of δ is sometimes considered to be about two thirds of the backfill friction angle ϕ (i.e., $\delta \approx 2\phi/3$) (Bowles 1996, Becker and Moore 2006). For typical mine stopes with rough walls, the value of δ is expected to be close to the friction angle of backfill ($\delta \approx \phi$) because shearing mostly takes place within the backfill itself (Aubertin *et al.* 2003, Li *et al.* 2003, Singh *et al.* 2010).

Fig. 3 shows an isolated circular arc element (with acting compressive stresses) with the normal (F_n) and shear (F_s) contact forces between the backfill and walls. F_z and $F_z + dF_z$ are the vertical forces acting on the upper and lower faces of the arc element, respectively. The weight of the arc element is

$$dW = 2\,\gamma\,\omega_w\,R\,dz = 2\,\gamma\,\omega_w\,B\,\kappa\,dz \tag{15}$$

The resulting force (F_z) acting on the upper face of the arc element is

$$F_z = \int_{-\omega_w}^{+\omega_w} (\sigma_1 R\,\cos\omega)\,d\omega \tag{16}$$

Integration of Eq. (16) gives

$$F_z = 2R\,\sigma_1\sin\omega_w \tag{17}$$

Substituting Eq. (4) into Eq. (17) gives

$$F_z = 2B\kappa\,\sigma_1\sin\omega_w \tag{18}$$

and

$$dF_z = 2B\kappa\,d\sigma_1\sin\omega_w \tag{19}$$

The force acting on the lower face of the arc element is

$$F_z + dF_z = 2B\,\kappa\,(\sigma_1 + d\sigma_1)\,\sin\omega_w \tag{20}$$

Considering the equilibrium of the arc element in the vertical direction leads to

$$dF_z = dW - 2F_s \tag{21}$$

The shear force provided by the shear strength along the walls, *Fs* on the arc (Fig. 3) can be expressed as

$$F_s = \tau_{sw}\,dz_w = \left[\sigma_1\left(\sin^2\omega_w + K_{ps}\cos^2\omega_w\right)\tan\delta\right]\frac{dz}{\cos\omega_w} \tag{22}$$

where dz_w $(= d_z/\cos\omega_w)$ is the apparent (vertical) thickness of the circular arc element at the contact with the wall.

Substituting Eqs. (15), (19) and (22) into Eq. (21) gives

$$\frac{P\ \mathrm{d}\sigma_1}{Q-\ \sigma_1 S}=\mathrm{d}z \qquad (23)$$

where P, Q and S can be expressed as follows

$$P=\ B\ \kappa \sin\omega_w \qquad (24)$$

$$Q=\gamma\ B\kappa\ \omega_w \qquad (25)$$

$$S=\frac{\tan\delta}{\cos\omega_w}\left(\sin^2\omega_w+K_{ps}\cos^2\omega_w\right) \qquad (26)$$

Solving Eq. (23) leads to the following expression for the major principal stress σ_1 along the circular arc

$$\sigma_1=\frac{Q}{S}\left[1-\exp\left(-\frac{S}{P}z\right)\right] \qquad (27)$$

The minor principal stress σ_3 along the circular arc can then be obtained by Eq. (11).

Eq. (27) with Eqs. (11), (24) to (26) constitute an analytical solution for the principal stresses in a vertical backfilled opening along an arc.

Considering point *C* on the circular arc, defined by (x, y) in the global coordinates system and (X, Y) or $(X,\ \omega)$ in the local system, the vertical distance EG (see Fig. 2) can be calculated as follows

$$EG=R(1-\cos\omega) \qquad (28)$$

Here, $X = x$ and y can be related to z as follows

$$z=y-EG=y-R(1-\cos\omega) \qquad (29)$$

Substituting Eq. (7) into Eq. (29) leads to

$$z=y-\left[B\kappa\left(1-\sqrt{1-\left(\frac{x}{B\kappa}\right)^2}\right)\right]=y-\left[B\kappa-\sqrt{(B\kappa)^2-x^2}\right] \qquad (30)$$

The major principal stress σ_1 at point *C* defined in the global coordinates system (x, y) within the backfilled stope can then be expressed as follows

$$\sigma_{1(x,y)}=\frac{Q}{S}\left\{1-\exp\left(-\frac{S}{P}\left(y-\left[B\kappa-\sqrt{(B\kappa)^2-x^2}\right]\right)\right)\right\} \qquad (31)$$

Eqs. (11) and (31) can then be used to evaluate the principal stresses at any point $(x,\ y)$ in the backfilled opening. The vertical and horizontal normal stresses at any point (x, y) can then be written as

$$\sigma_{v(x,y)}=\sigma_{1(x,y)}\left[\frac{1+K_{ps}}{2}+\frac{1-K_{ps}}{2}\cos\left(2\sin^{-1}\left(\frac{x}{B\kappa}\right)\right)\right]=\sigma_{1(x,y)}\left[1-\left(1-K_{ps}\right)\left(\frac{x}{B\kappa}\right)^2\right] \qquad (32)$$

$$\sigma_{h(x,y)}=\sigma_{1(x,y)}\left[\frac{1+K_{ps}}{2}-\frac{1-K_{ps}}{2}\cos\left(2\sin^{-1}\left(\frac{x}{B\kappa}\right)\right)\right]=\sigma_{1(x,y)}\left[K_{ps}+\left(1-K_{ps}\right)\left(\frac{x}{B\kappa}\right)^2\right] \qquad (33)$$

4. Proposed solution for calculating the stresses in vertical backfilled openings

Radius R can considerably affect the calculated vertical and horizontal stresses in the stope. When the backfill has little friction (i.e. $\phi\approx 0$), the arching effect is largely absent and radius R is expected to approach infinity. But this is not the case with Eqs. (4) and (5), which predict a finite value of $R=\sqrt{2}B$ for $\phi\approx 0°$. A modification is

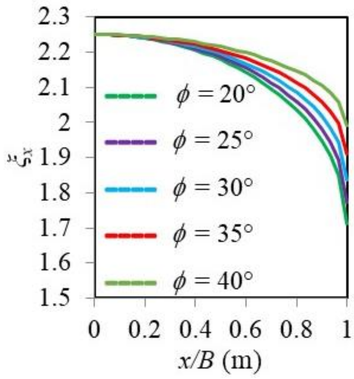

(a) 2*B* = 3 m and *H* = 45 m

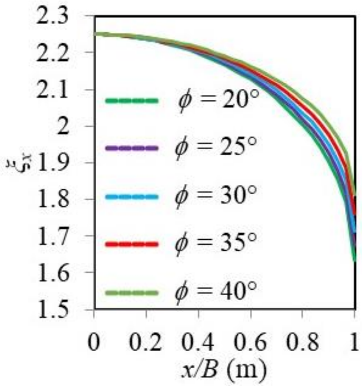

(b) 2*B* = 18 m and *H* = 45 m

Fig. 4 Variation of the correction factor ξ_x as a function of (*x/B*) for different friction angles ϕ and different stope height *H*

made here by replacing R with $\xi_x R$ (and $B\kappa$ with $\xi_x B\kappa$), where ξ_x is a unit-less correction factor that serves to better define the influence of the radius R, and the effect of the internal friction angle ϕ (Eqs. (4) and (5)). Eqs. (24) and (25) then become

$$P'=\xi_x\ B\ \kappa\ \left[\sin\omega_w\right] \qquad (34)$$

$$Q'=\ \gamma\ \xi_x\ B\kappa\ \omega_w \qquad (35)$$

The principal major stress at any point (x, y) within the backfilled stope can then be expressed as follows

$$\sigma_1=\frac{Q'}{S}\left[1-\exp\left(-\frac{S}{P'}\left(y-\left[\xi_x\ B\kappa-\sqrt{(\xi_x\ B\kappa)^2-x^2}\right]\right)\right)\right] \qquad (36)$$

The vertical and horizontal normal stresses at any point (x, y) in the backfilled opening becomes

$$\sigma_{v(x,y)}=\sigma_1\left[1-\left(1-K_{ps}\right)\left(\frac{x}{\xi_x\ B\kappa}\right)^2\right] \qquad (37)$$

$$\sigma_{h(x,y)}=\sigma_1\left[K_{ps}+\left(1-K_{ps}\right)\left(\frac{x}{\xi_x\ B\kappa}\right)^2\right] \qquad (38)$$

The earth pressure coefficient at any point (x, y) within the backfilled stope can thus be expressed as follows

$$K=K_{(x,y)}=\sigma_{h(x,y)}/\sigma_{v(x,y)}=\frac{K_{ps}+\left(1-K_{ps}\right)\left(\frac{x}{\xi_x\ B\kappa}\right)^2}{1-\left(1-K_{ps}\right)\left(\frac{x}{\xi_x\ B\kappa}\right)^2} \qquad (39)$$

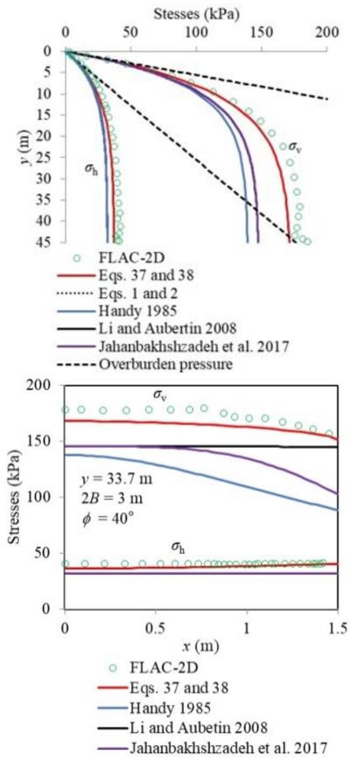

(a)

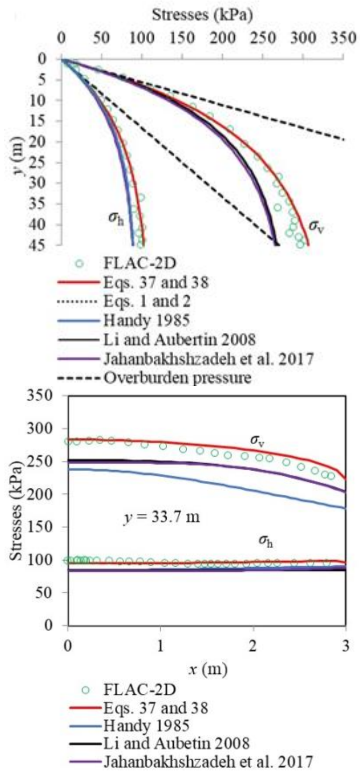

(b)

Fig. 5 Illustration of the various solutions, based on the e horizontal and vertical normal stresses along the VCL (x = 0 m) of a stope having a fill height of H=45 m and across the stope width at a depth y = 33.7 m, obtained by the proposed solution (Eqs. (34)-(41)) and other analytical solutions, and also those given by numerical simulations (a) for 2B = 3 m with ϕ = 40° and (b) for 2B = 6 m with ϕ = 30°

As can be seen, this earth pressure coefficient K depends on position x, but not on y. A similar approach has been proposed by Jahanbakhshzadeh *et al.* (2017a, b), but with a different type of solution.

Numerical results obtained by Li and Aubertin (2008), with additional simulations performed here, have been used to determine the value of the correction factor ξ_x for a variety of conditions. Applying a curve fitting technique to the numerical results leads to the following expression for factor ξ_x

$$\xi_x = \left[\eta + (2.25 - \eta)\sqrt{1 - \left(\frac{x}{B}\right)^2}\right]\tan^{0.25}\phi \tag{40}$$

where η is defined as follows

$$\eta = 1.5 + 0.25\left(\frac{H}{B}\right)^{0.25}\tan\phi \tag{41}$$

Fig. 4 shows the variation of the correction factor ξ_x as a function of (x/B) for different friction angles for narrow (Fig. 4(a)) and wide (Fig. 4(b)) stopes. One sees that the value of ξ_x, remains constant along the centerline, but tends to increase near the wall with the internal friction angle.

Eqs. (34)-(41) constitute the proposed analytical solution for estimating the horizontal and vertical stresses in vertical backfilled opening at any point (x, y) within the backfilled stope.

5. Assessment of the proposed solution using numerical simulations

As mentioned above, some of the numerical results obtained by Li and Aubertin (2008) have been used to obtain Eqs. (40) and (41) through a calibration process (i.e. adjustment of parameters to obtain a good agreement between the proposed solution and numerical results). An illustration of this calibration is shown in Fig. 5 for the horizontal and vertical normal stresses along the VCL (x = 0 m) and across the width of the stope at a depth y = 33.7 m; these results were obtained from the proposed solution (Eqs. (34)-(41)) and compared with those provided by Li and Aubertin (2008) (following simulations with FLAC-2D, Itasca 2002). In these calculations, the backfill has a height of H = 45 m. The first calculation was made with ϕ = 40° and 2B = 3m (Fig. 5(a)) and the second with ϕ = 30° and 2B = 6 m (Fig. 5(b)). The horizontal to vertical stresses based on the analytical solutions of Handy (1985), Li and Aubertin (2008) and Jahanbakhshzadeh *et al.* (2017) as well as the overburden solution ($\sigma_v = \gamma y$ and $\sigma_h = K_0\sigma_v$, with K_0 given by Jaky's equation) have also been plotted on the same figure. It can be seen that the vertical and horizontal normal stresses obtained by the proposed solution (Eqs. (34)-(41) using $K_{ps} = K_a$) are very close to those obtained from numerical modeling. An improvement is obtained compared to the other existing solutions. In all cases, the calculated stresses are much lower than those based on the overburden solution.

To test the flexibility of the proposed analytical solution and its ability to predict representative stresses for other conditions, additional numerical simulations have been

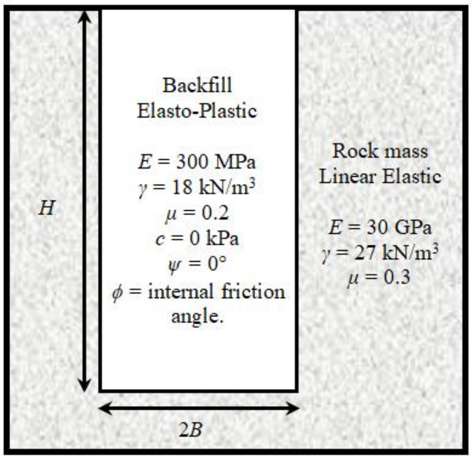

(a) Physical model (adapted from Li *et al.* 2003)

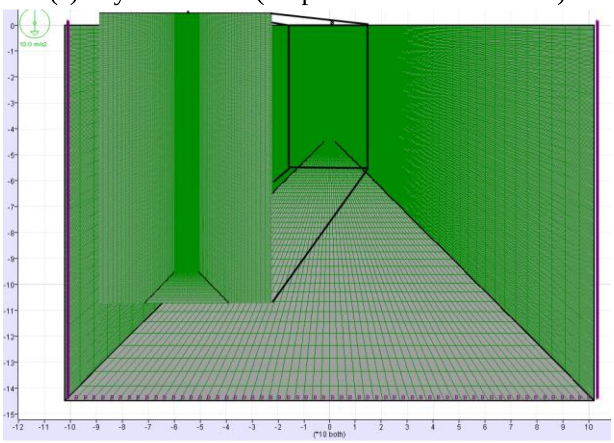

(b) Numerical model

Fig. 6 Physical and numerical models used for the additional simulation conducted to test the proposed solution.

Table 1 Numerical simulations performed with FLAC-2D (calculations made with γ = 18 kN/m^3, μ= 0.2, E = 300 MPa, c = 0 kPa and ψ = 0°)

Cases	Figures	2B (m)	ϕ (°)	H (m)
1	7, 8, 9	4.5	35	45
2	10		25	
3	11a	15	38	
4	11b	10	33	
5	12a	8	37	80
6	12b		32	20

conducted with FLAC-2D (Itasca 2002). Fig. 6 shows the physical (Fig. 6(a)) and numerical (Fig. 6(b)) models for a stope having a width 2B = 4.5 m, filled to a height of H = 45 m. The rock mass is considered homogeneous, isotropic, and linearly elastic. It has a Young's modulus of E = 30 GPa; a Poisson's ratio of μ = 0.3 and a unit weight of γ = 27 kN/m^3. The backfill is assumed to be elasto-plastic obeying the Mohr-Coulomb criterion. It is characterized by a unit weight of γ = 18 kN/m^3, a Young's modulus of E = 300 MPa, a Poisson's ratio of μ = 0.2, and a varying internal friction angle ϕ; both the cohesion c (= 0) and dilation

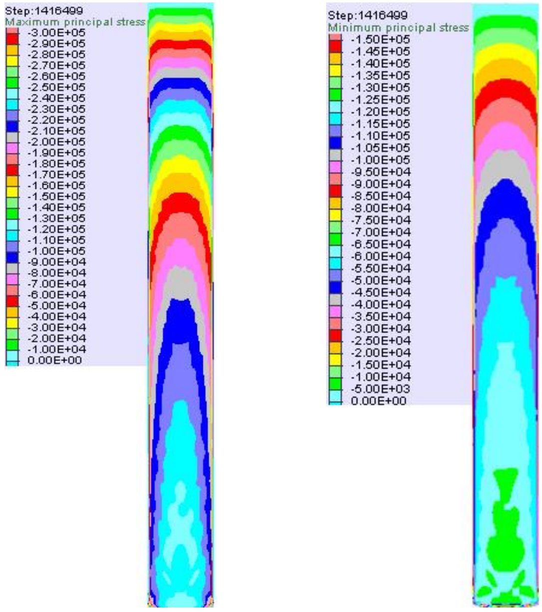

(a) Major principal stresses (b) Minor principal stresses

Fig. 7 Iso-contours of the major and minor principal stresses (negative in compression) in the backfilled stope provide by the simulation with FLAC-2D for Case 1 (see details in Table 1).

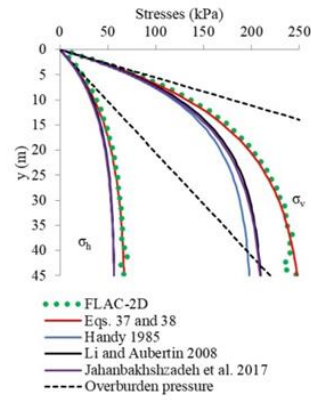

(a)

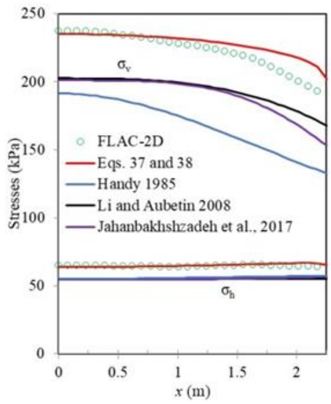

(b)

Fig. 8 Illustration of the various solutions, based on the horizontal and vertical normal stresses (a) along the VCL and (b) across the width at y = 33.7 m, obtained by the proposed solution (Eqs. (34)-(41)), and other analytical solutions, and also those given by numerical simulations for Case 1 (ϕ = 35°, 2B = 4.5 m, H = 45 m), Table 1

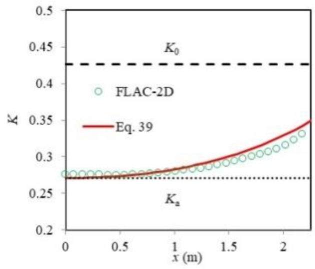

(a) y = 22.5 m

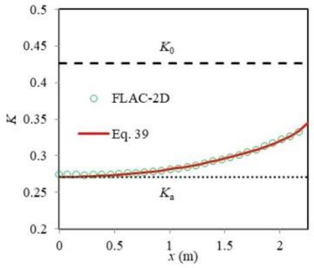

(b) y = 33.7 m

Fig. 9 Variation of the horizontal to vertical normal stress ratio $K(=\sigma_h/\sigma_v)$ across the half-width of a stope at (a) a depth of y = 22.5 m and (b) another depth of y = 33.7 m, obtained by the proposed solution (Eq. (39)) and numerical simulations for Case 1 (ϕ = 35°, 2B = 4.5 m, H = 45 m), Table 1

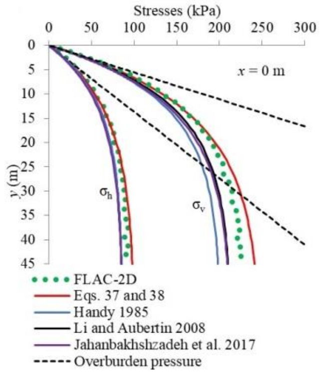

(a)

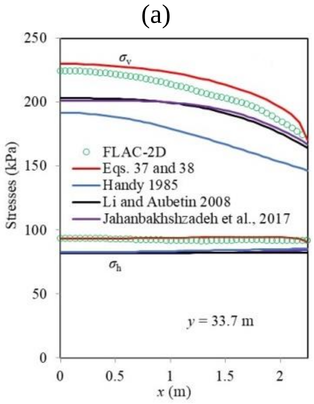

(b)

Fig. 10 Illustration of the various solutions, based on the horizontal and vertical normal stresses (a) along the VCL and (b) across the width of the stope at a depth of y = 33.7 m, obtained by the proposed solution (Eqs. (34)-(41)) and other analytical solutions, and also those given by numerical simulations for Case 2 (ϕ = 25°, 2B = 4.5 m, H = 45 m), Table 1

angle ψ (= 0) are nil. The boundaries conditions at the base and along the two sides (rock mass) are fixed in all directions. The stope is filled sequentially with 15 layers (3 m thick each). The cases covered by the numerical simulations are shown in Table 1.

Fig. 7 shows the distributions of the major (Fig. 7(a)) and minor (Fig. 7(b)) principal stresses in the backfilled stope given by the numerical simulation with FLAC-2D for Case 1 (Table 1). One sees that the stresses are higher at the center of the stope than near the walls. They increase (almost) linearly with the depth near the surface of the backfill but tends to become constant at large depth (see also following figures). These are typical indicators of an arching effect (Aubertin *et al.* 2003, Li *et al.* 2003). It is also seen that the curvature of the iso-contours tends to change with depth; the aspect is not taken into account with the proposed solution, as will be discussed below.

Fig. 8 shows the variation of the horizontal and vertical normal stresses along the VCL (Fig. 8(a)) and across the width of the stope at a depth of y = 33.7 m (Fig. 8(b)), obtained from the proposed solution (Eqs. (34)-(41)) and numerical simulation for Case 1. The figure also shows the stresses calculated with other existing solutions based on the overburden or an arching effect. One sees that the agreement between the numerical results and those

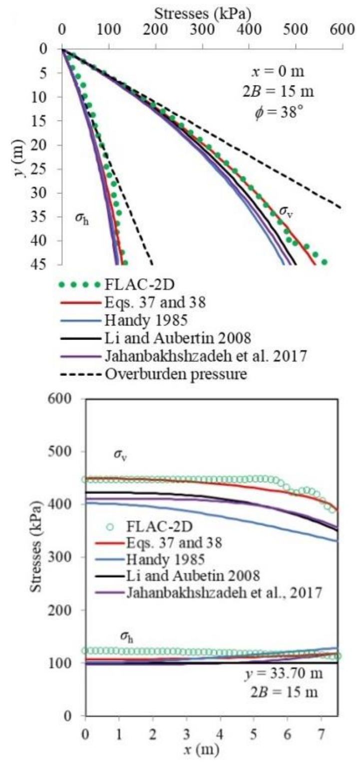

(a)

Fig. 11 Illustration of the various solutions, based on the horizontal and vertical normal stresses and along the VCL (upper graphs) and across the width (lower graphs) of the stope at a depth of y = 33.7 m, obtained by the proposed solution (Eqs. (34)-(41)) and other analytical solutions, and also those given by numerical simulations: (a) for Case 3 (ϕ = 38°, 2B = 15 m and H = 45 m), Table 1 and (b) for Case 4 (ϕ = 33°, 2B = 10 m and H = 45 m), Table 1

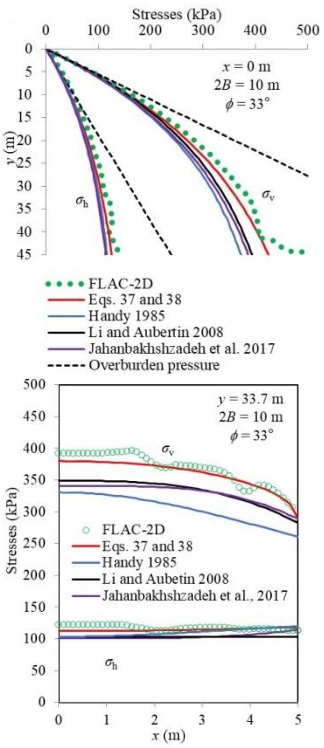

(b)

Fig. 11 Continued

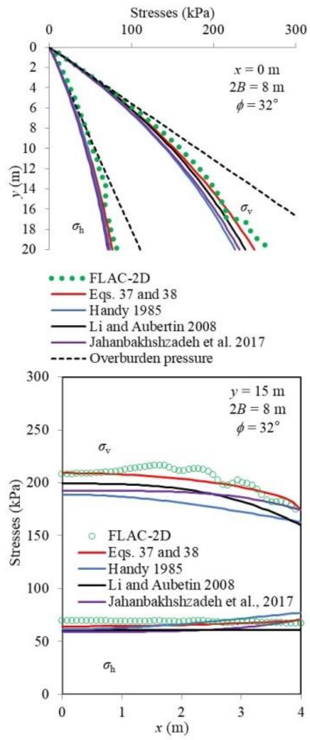

(b)

Fig. 12 Continued

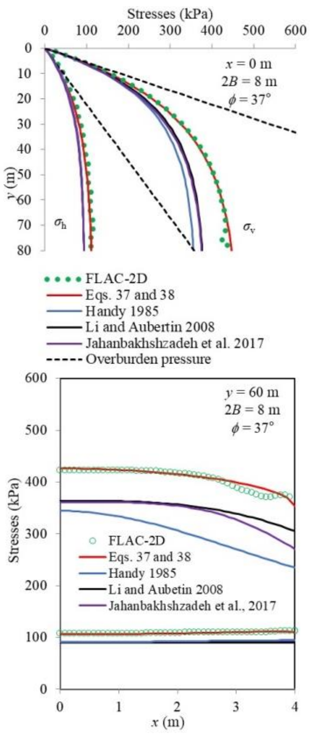

(a)

Fig. 12 Illustration of the various solutions, based on the horizontal and vertical normal stresses along the VCL (upper graphs) and across the width (lower graphs) of the stope at a given depth, obtained by the proposed solution (Eqs. (34)-(41)) and other analytical solutions, and also those given by numerical simulations: (a) for Case 5 (ϕ = 37°, $2B$ = 8 m and H = 80 m), Table 1 and (b) for Case 6 (ϕ = 32°, $2B$ = 8 m and H = 20 m), Table 1

predicted by the proposed solution (Eqs. (34) to (41) using $K_{ps} = K_a$) is excellent. There is an improved correlation with the simulation compared with the other solutions.

Fig. 9 shows the variation of the horizontal to vertical normal stress ratio K across the half-width of a stope at a depth of y = 22.5 m (Fig. 9(a)) and another depth of y = 33.7 m (Fig. 9(b)), obtained by the proposed analytical solution (Eqs. (39) to (41)) and numerical modeling with FLAC-2D. The figures indicate that the proposed solution captures the non-uniform distribution across the width of the stope.

Figs. 10 to 12 shows the variation of the horizontal and vertical normal stresses along the VCL (upper graphs) and across the width (lower graphs) of the stope at a given depth, provided by the proposed solution (Eqs. (34) to (41)) and by simulations with FLAC-2D, considering ϕ = 25°, $2B$ = 4.5 m and H = 45 m (Fig. 10, Case 2, Table 1), ϕ = 33°, $2B$ = 10 m and H = 45 m (Fig. 11(a), Case 3, Table 1), ϕ = 38°, $2B$ = 15 m and H = 45 m (Fig. 11(b), Case 4, Table 1), ϕ = 37°, $2B$ = 8 m and H = 80 m (Fig. 12(a), Case 5, Table 1), and ϕ = 32°, $2B$ = 8 m and H = 20 m (Fig. 12(b), Case 6, Table 1). One sees that there is a good agreement between the numerical results and those given by the proposed solution, in all cases. This suggests that the proposed solution could be used to estimate the stresses in vertical backfilled openings.

6. Discussion

A modified analytical solution has been developed for the stresses in backfilled stopes based on a circular arc distribution. It gives the vertical and horizontal stresses at any position in the opening. An expression has also been obtained for the horizontal to vertical stress ratio, $K(=\sigma_h/\sigma_v)$. There is a good agreement between the proposed solution and numerical modeling results, in terms of the vertical and horizontal stresses and earth pressure coefficient along the VCL and across the width of the opening. Additional improvements to this solution can still be made by considering the following aspects:

• In this paper, the radius R of the circular arc element was considered as a constant, as proposed by Harrop-Williams (1989) and Singh *et al.* (2011). This may not reflect the real response of fill placed in a confined opening. Rather, it can be expected that this radius may change with depth, particularly near the surface of the backfill. This trend can be seen from the iso-contours of the major (Fig. 7(a)) and minor (Fig. 7(b)) principal stresses obtained by numerical modeling.

• The numerical results showed that K is equal to K_a at the center line and close to the K_o near the walls. These simulation results were obtained by considering the Poisson's ratio (μ) and internal friction angle (ϕ) of the backfill as two independent parameters. Complementary work has also been done to investigate the stresses in backfilled stope by considering interrelated μ and ϕ to obtain a unique and consistent earth pressure coefficient at rest K_o (e.g., Falaknaz *et al.* 2015, Jahanbakhshzadeh *et al.* 2017). This assumption could also be adopted for the analytical solution developed here.

• The proposed solution assumes that the earth pressure coefficient changes across the width of the stope, but remains constant with depth. Numerical results (Li and Aubertin 2015, Yang *et al.* 2017a) and in situ measurements (Thomson *et al.* 2012) have shown that the K value could also depend on depth.

• Improvements can also be considered by taking into account a different shape for the arc, and other factors including water pressures, cohesion, and proprieties of the interfaces along the fill-wall contact. This is particularly the case for barricade design, for which the most critical time is shortly after the placement of a fresh backfill containing relatively large amount of water (Li and Aubertin 2019c, d, Komurlu and Kesimala 2015, Yang *et al.* 2017b).

• Additional laboratory and field measurements to validate (or calibrate) the proposed model and analytical solutions would also be welcome.

7. Conclusions

An analytical solution was developed by considering a circular arc element to evaluate the stresses in vertical backfilled openings. The analytical solution includes a varying radius for the circular element. The validity of the proposed solution has been evaluated using a large number of numerical modeling results. The good agreement between the analytical solution and the numerical simulations, in terms of earth pressure coefficient and stresses, indicate that this solution can be useful to estimate the stresses in backfilled openings.

Acknowledgements

The authors would like to acknowledge the financial support from the Natural Sciences and Engineering Research Council of Canada (NSERC), Institut de recherche Robert-Sauvé en santé et en sécurité du travail du Québec (IRSST), Fonds de recherche du Québec-Nature et Technologies (FRQNT), and industrial partners of the Research Institute on Mines and the Environment (RIME UQAT-Polytechnique; http://rime-irme.ca/).

References

Askew, J., McCarthy, P.L and Fitzgerald, D.J. (1978), "Backfill research for pillar extraction at ZC/NBHC", *Proceedings of the 12th Canadian Rock Mechanics Symposium*, Sudbury, Canada.

Atkinson, J.H., Cairncross, A.M. and James, R.G. (1974), "Model tests on shallow tunnels in sand and clay", *Tunn. Tunn.*, **6**(4), 28-32.

Aubertin, M. (1999), "Application de la mécanique des sols pour l'analyse du comportement des remblais miniers souterrains", *Proceedings of the Short Course Lecture Notes, 14th Ground Control Conference*, Val-d'Or, Québec,Canada, March.

Aubertin, M., Bernier, L. and Bussière, B. (2002), *Environnement et Gestion des Rejets Miniers*, Presse Internationale Polytechnique, Montreal, Canada.

Aubertin, M., Li, L., Arnoldi, S., Belem, T., Bussière, B., Benzaazoua, M. and Simon, R. (2003), "Interaction between backfill and rock mass in narrow stopes", *Proceedings of the Soil and Rock America 2003*, Cambridge, Massachusetts, Cambridge, Massachusetts, U.S.A., June.

Das, B.M. (1998), *Principles of Geotechnical Engineering-Equivalent Hydraulic Conductivity in Stratified Soil*, PSW.

Becker, D.E. and Moore, I.D. (2006), *Canadian Manual of Foundation Engineering*, Canadian Geotechnical Society, Canada.

Blight, G.E. (1984), "Soil mechanics principals in underground mining", *Geotechnique*, **110**(5), 567-581.

Bowles, J.E. (1996), *Foundation Analysis and Design*, McGraw-Hill.

Cowin, S.C. (1977), "The theory of static loads in bins", *J. Appl. Mech.*, **44**(3), 409-412.

Dalvi, R.S. and Pise, P.J. (2008), "Effect of arching on passive earth pressure coefficient", *Proceedings of the 12th International Conference of International Association for Computer Methods and Advances in Geomechanics (IACMAG)*, Goa, India, October.

De Souza, E. and Dirige, A.P.E. (2002), "Arching effects and sillmat behaviour", *Proceedings of the 104th Annual General Meeting of the Canadian Institute of Mining Metallurgy and Petroleum*, Vancouver, B.C., Canada, May.

Falaknaz, N., Aubertin, M. and Li, L. (2015), "Numerical investigation of the geomechanical response of adjacent backfilled stopes", *Can. Geotech. J.*, **52**(10), 1507-1525.

Goel, S. and Patra, N.R. (2008), "Effect of arching on active earth pressure for rigid retaining walls considering translation mode", *J. Geomech.*, **8**(2), 123-133.

Handy, R.L. (1985), "The arch in soil arching", *J. Geotech. Eng.*, **111**(3), 302-318.

Harrop-Williams, K.O. (1989), "Geostatic wall pressures", *J. Geotech. Eng.*, **115**(9), 1321-1325.

Hartlen, J., Nielsen, J., Ljunggren, L., Martensson, G. and Wigram, S. (1984), *The Wall Pressure in Large Grain Silos*, Swedish Council for Building Research, Stockholm, Sweden.

Itasca. (2002), *Itasca Consulting Group Inc. User's Guide, Theory and Background*, Fast Lagrangian Analysis of Continua,

Minneapolis, Minnesota, U.S.A.
Jahanbakhshzadeh, A., Aubertin, M. and Li, L. (2017), "A new analytical solution for the stress state in inclined backfilled mine stopes", *Geotech. Geol. Eng.*, **35**(3), 1151-1167.
Jaky, J. (1944), "The coefficient of earth pressure at rest", *J. Soc. Hungarian Arch. Eng.*, **7**, 355-358.
Janssen, H.A. (1895), "Versuche uber getreidedruck in silozellen", *Z. Ver. Dtsch. Ing.*, **39**, 1045-1049.
Knutsson, S. (1981), "Stresses in the hydraulic backfill from analytical calculations and in-situ measurements", *Proceedings of the Conference on the Application of Rock Mechanics to Cut and Fill Mining*, Lulea, Sweden, June.
Komurlu, E. and Kesimala, A. (2015), "Sulfide-rich mine tailings usage for short-term support purposes: An experimental study on paste backfill barricades", *Geomech. Eng.*, **9**(2), 195-205.
Kutzner, C. (1997), *Earth and Rockfill Dams: Principles of Design and Construction*, CRC Press.
Ladanyi, B. and Hoyaux, B. (1969), "A study of the trap-door problem in a granular mass", *Can. Geotech. J.*, **6**(1), 1-14.
Li, L, Aubertin, M. and Belem, T. (2005), "Formulation of a three-dimensional analytical solution to evaluate stress in backfilled vertical narrow openings", *Can. Geotech. J.*, **42**(6), 1705-1717.
Li, L. and Aubertin, M. (2008), "An improved analytical solution to estimate the stress state in sub-vertical backfilled stopes", *Can. Geotech. J.*, **45**(10), 1487-1496.
Li, L. and Aubertin, M. (2009a), "Influence of water pressure on the stress state in stopes with cohesionless backfill", *Geotech. Geol. Eng.*, **27**(1), 1-11.
Li, L. and Aubertin, M. (2009b), "A three-dimensional analysis of the total and effective stresses in submerged backfilled stopes", *Geotech. Geol. Eng.*, **27**(4), 559-569.
Li, L. and Aubertin, M. (2009c), "Horizontal pressure on barricades for backfilled stopes. Part I: Fully drained conditions", *Can. Geotech. J.*, **46**(1), 37-46.
Li, L. and Aubertin, M. (2009d), "Horizontal pressure on barricades for backfilled stopes. Part II: Submerged conditions", *Can. Geotech. J.*, **46**(1), 47-56.
Li, L. and Aubertin, M. (2015), "Numerical analysis of the stress distribution in symmetrical backfilled trenches with inclined walls", *Ind. Geotech. J.*, **45**(3), 278-290.
Li, L., Aubertin, M., Shirazi, A., Belem, T. and Simon, R. (2007), "Stress distribution in inclined backfilled stopes", *Proceedings of the 9th International Symposium in Mining with Backfill*, Montreal, Canada, April-May.
Li, L., Aubertin, M., Simon, R., Bussière, B. and Belem, T. (2003), "Modeling arching effects in narrow backfilled stopes with FLAC", *Proceedings of the 3rd International Symposium on FLAC and Numerical Modeling in Geomechanics*, Subury, Canada, October.
Marston, A. (1930), *The Theory of External Loads on Closed Conduits in the Light of Latest Experiments*, Bulletin No. 96, Iowa Engineering Experiment Station, Iowa State College, Ames, Iowa, U.S.A.
McCarthy, D.F. (1988), *Essentials of Soil Mechanics and Foundations: Basic Geotechnics*, Upper Saddle River, Prentice Hall, New Jersey, U.S.A.
McCarthy, D.F. (1993), *Essentials of Soil Mechanics and Foundations: Basic Geotechnics*, 4th Edition, Prentice Hall Books.
Moradi, G. and Abbasnejad, A. (2015), "Experimental and numerical investigation of arching effect in sand using modified Mohr Coulomb", *Geomech. Eng.*, **8**(6), 829-844.
Ning, J., Wang, J., Tan, Y., Zhang, L. and Bu, T. (2017). "In situ investigations into mining-induced overburden failures in close multiple-seam longwall mining: A case study", *Geomech. Eng.*, **12**(4), 657-673.
Ono, K. and Yamada, M. (1993), "Analysis of arching action in granular mass", *Geotechnique*, **43**(1), 105-120.
Ooi, J.Y. and Rotter, J.M. (1990), "Wall pressures in squat steel silos from simple finite element analysis", *Comput. Struct.*, **37**(4), 361-374.
Paik, K.H. and Salgado, R. (2003), "Estimation of active earth pressure against rigid retaining walls considering arching effects", *Geotechnique*, **53**(7), 643-653.
Pirapakaran, K. and Sivakugan, N. (2006), "Numerical and experimental studies of arching effects within mine fill slopes", *Proceedings of the 6th International Conference on Physical Modelling in Geotechnics*, Hong Kong, August.
Pirapakaran, K. and Sivakugan, N. (2007a), "A laboratory model to study arching within a hydraulic fill stope", *Geotech. Test. J.*, **30**(6), 496-503.
Pirapakaran, K. and Sivakugan, N. (2007b), "Arching within hydraulic fill stopes", *Geotech. Geol. Eng.*, **25**(1), 25-35.
Singh, S., Shukla, S.K. and Sivakugan, N. (2011), "Arching in inclined and vertical mine stopes", *Geotech. Geol. Eng.*, **29**(5), 685-693.
Sobhi, M.A., Li, L. and Aubertin, M. (2017), "Numerical investigation of earth pressure coefficient along central line of backfilled stopes", *Can. Geotech. J.*, **54**(1), 138-145.
Sokolovoski, V.V. (1965), *Statics of Granular Media*, Pergamon Press, Oxford, U.K.
Spangler, M.G. (1962), *Section 11: Culverts and Conduits. Foundation Engineering*, McGraw-Hill, New York, U.S.A.
Take, W.A. and Valsangkar, A.J. (2001), "Earth pressures on unyielding retaining walls of narrow backfill width", *Can. Geotech. J.*, **38**(6), 1220-1230.
Terzaghi, K. (1943), *Theoretical Soil Mechanics*, Wiley, New York, U.S.A.
Thompson, B.D., Grabinsky, M.W. and Bawden, W.F. (2012), "In situ measurements of cemented paste backfill at Cayeli Mine", *Can. Geotech. J.*, **49**(7), 755-772.
Ting, C.H., Sivakugan, N., and Shukla, S.K. (2012), "Laboratory simulation of the stresses within inclined stopes", *Geotech. Test. J.*, **35**(2), 280-294.
Yang, P., Li, L. and Aubertin, M. (2017a), "Stress ratios in entire mine stopes with cohesionless backfill: A numerical study", *Minerals*, **7**(10), 201.
Yang, P.Y., Li, L., Aubertin, M., Brochu-Baekelmans, M. and Ouellet, S. (2017b), "Stability analyses of waste rock barricades designed to retain paste backfill", *Int. J. Geomech.*, **17**(3), 04016079.

CC